ELSEVIER

Thermochimica Acta 334 (1999) 39–47

thermochimica acta

www.elsevier.com/locate/tca

Thermal characterization of acrylic-based latex blend films by modulated and pulsed differential scanning calorimetry

N. Agarwal[1], R.J. Farris*

Polymer Science and Engineering Department, Silvio O. Conte National Center for Polymer Research, University of Massachusetts, Amherst, MA 01003, USA

Received 19 June 1998; accepted 27 May 1999

Abstract

A complete thermal characterization of acrylic-based latex blend films is presented here using thermogravimetric analysis (TGA), modulated differential scanning calorimetry (MDSC) and pulsed differential scanning calorimetry (pulsed-DSC). These blend films are prepared from aqueous-based latices of poly(methyl methacrylate-co-ethyl acrylate) and poly(methyl methacrylate-co-butyl acrylate). The copolymer compositions are controlled to yield glass transition temperatures, T_g, of 45°C and −5°C, respectively. The presence of two distinct glass transition temperatures at all compositions confirm the phase separated nature of these blends. There is partial miscibility at intermediate compositions arising from significant segmental inter-diffusion across the particle interface. Constant temperature pulsed-DSC experiments, as well as those through the T_g, yield a rate-independent specific heat profile for these blends.

Keywords: Equilibrium specific heat; DSC; MDSC; Complex heat capacity; Pulsed-DSC; Glass transition; Blend miscibility

1. Introduction

Thermal characterization of a material involves measurement of its thermal stability, temperatures and heats of thermal transitions. Thermogravimetric analysis (TGA) and differential scanning calorimetry (DSC) are standard techniques used to measure the thermal behavior of polymers.

Recently modulated DSC [1] has gained widespread popularity due to increased sensitivity and resolution of measurement. The main difference, compared to conventional DSC, is that the usual input heating (or cooling) temperature ramp is ''modulated'' by superimposing a small sinusoidal perturbation. The temperature profile is then given by

$$T(t) = T_0 + \beta_0 t + T_a \sin(\omega_0 t), \quad (1)$$

where T_0 is the initial temperature, β_0 the heating (or cooling rate), T_a is the amplitude of sinusoidal temperature change of frequency ω_0.

The resulting heat flux is also a sine function, out-of-phase with the input, riding on an underlying non-oscillating ''average'' flux, ϕ_{dc}

$$\phi(t) = \phi_{dc} + \phi_a \sin(\omega_0 t + \varphi), \quad (2)$$

where ϕ_a and φ are the amplitude and phase lag of the output heat flux. The underlying heat flux is the same as that measured in an identical DSC experiment

*Corresponding author. Tel.: +1-413-577-3125; fax: +1-413-545-0082

E-mail address: rjfarris@polysci.umass.edu (R.J. Farris)

[1]Present address: Corporate New Business and Technology, Kimberly–Clark Corporation, 1400 Holcomb Bridge Road, Roswell, GA 30076-2199, USA., nagarwal@kcc.com

0040-6031/99/$ – see front matter
PII: S0040-6031(99)00125-2

without the sinusoidal temperature variation. A fast Fourier analysis (FFT), described by Wunderlich and coworkers [2] and Wunderlich [3] enables separation of the non-oscillating flux from the oscillating component, as well as its amplitude and phase lag.

Two methods of analyzing the modulated heat flux and temperature data are reported in the literature. The first, due to Reading et al. [1], and adopted by TA Instruments in their DSC2910 modules, defines the in-phase component of the oscillating heat flux as the ''reversing'' heat flux

$$\phi_{\mathrm{rev}}(T,\omega_0) = |C(T,\omega_0)|\beta_0, \tag{3}$$

where $|C(T,\omega_0)|$ is the modulus of the frequency-dependent specific heat of the material that is available from the amplitudes of oscillating heat flux, temperature and frequency

$$|C(T,\omega_0)| = K_C \frac{\phi_{\mathrm{a}}}{\omega_0 T_{\mathrm{a}}}, \tag{4}$$

where K_C is the specific heat constant obtained from calibrations with a sapphire standard. A ''non-reversing'' heat flux is then calculated as

$$\phi_{\mathrm{non-rev}}(T,\omega_0) = \phi_{\mathrm{dc}} - \phi_{\mathrm{rev}}. \tag{5}$$

The second method, due to Schawe [4], treats the non-oscillating, ϕ_{dc}, and the oscillating component of the heat flux as two mathematically disparate quantities. The oscillating part of the heat flux yields a complete description of the frequency-dependent specific heat, $C(T,\omega_0)$ in terms of the in-phase and out-of-phase components:

$$|C(T,\omega_0)| = \sqrt{C'^2(T,\omega_0) + C''^2(T,\omega_0)} \tag{6}$$

whereas the phase shift is given by

$$\tan(\varphi) = \frac{C''(T,\omega_0)}{C'(T,\omega_0)}. \tag{7}$$

In a recent paper [5], we proposed a new pulsed-DSC technique that provides the time-independent equilibrium specific heat as well as a frequency-dependent complex specific heat in a single experiment. This approach is based on a simple moment analysis, followed by Fourier transform, of the input temperature perturbation and the resulting enthalpy change. The essential feature of this technique is the application of an input pulse of arbitrary shape and duration and collecting output data until the response has returned to its initial unperturbed base value. A simple Laplace analysis of the input and output data yields the equilibrium specific heat and a mean relaxation time, whereas the frequency-dependent quantities are calculated by Fourier transform. The main advantage of this method is that there is no restriction on the shape of the input perturbation. The only constraint is that both the input and the output must return to their initial unperturbed state at the end of the experiment; a requirement of the linear hereditary equations. A time-independent equilibrium specific heat is obtained from the areas under the temperature–time and enthalpy–time curves

$$C_{\mathrm{eq}}(T) = \frac{\int_0^\infty \Delta H(t)\,\mathrm{d}t}{\int_0^\infty \Delta T(t)\,\mathrm{d}t}. \tag{8}$$

Experiments on a variety of materials such as indium, copper, sapphire, amorphous and semi-crystalline polymers [5], have shown that the equilibrium specific heats obtained from pulsed-DSC experiments using Eq. (8) are indeed rate-independent. In the present work, we extend the pulsed-DSC measurements to span the entire glass transition for acrylic blends using a series of temperature pulses. These results are then compared with those obtained from MDSC.

2. Experimental

2.1. Materials

Methylmethacrylate-based copolymer latices were synthesized by Dr. G.D. Andrews of DuPont. The first latex was poly(methyl methacrylate-co-ethyl acrylate), P(MMA-co-EA), with a T_{g} of 45°C, and the second poly(methyl methacrylate-co-butyl acrylate), P(MMA-co-BA), with a T_{g} of −5°C. The co-monomer molar ratios in the two latices were 3 : 2 and 2 : 3, respectively, and these were stabilized by 0.35% and 0.17% (on molar basis) ammonium lauryl sulfate (ALS). Particle sizes of these latices, as measured by dynamic light scattering, were of the order of 100 nm. Unless mentioned otherwise, these two copolymers will be referred to as ''hard'' and ''soft'' in the subsequent description.

Blend films of the two copolymers were cast from the aqueous dispersions on a glass plate, dried at 70°C for 3–4 h and annealed at 130°C for 20 min. Films were easily removed from the glass plates with the aid of water. Time of exposure to water was minimized so as to limit the amount of absorbed water, and the excess water was wiped off from the surface with Kimwipes®. The films were later left to dry at room conditions. The composition of the blends was varied from 0% hard to 100% hard to obtain a complete set. A comprehensive characterization of the mechanical properties of these blends has been presented elsewhere [6].

2.2. TGA experiments on acrylic blends

TGA experiments were performed using a TGA2950 from TA Instruments with samples weighing around 5 mg under a nitrogen purge at a flowrate of 100 ml/min. A heating rate of 10°C/min was used to heat the samples from room temperature to approximately 400°C.

2.3. Modulated DSC measurements

For MDSC experiments on acrylic blend films, small pieces (20–30 mg) were cut from dried films and encapsulated in hermetically sealed aluminum pans. The weights of the sample and reference pans were matched to within 0.5 mg. MDSC experiments were carried out using a DSC2910 module from TA Instruments under a helium (He) purge at a flowrate of 80 ml/min. Calibrations for cell constant and specific heat were carried out using indium and sapphire standards, respectively. Each experiment involved cooling the sample from 90°C to −40°C at 2°C/min with a temperature amplitude of ±0.5°C and a period of oscillation of 40 s.

2.4. Pulsed-DSC measurements

Pulsed-DSC experiments were performed using a TA Instruments DSC2910 module. The instrument was first calibrated with indium and mercury for temperature and cell constant. Helium was used as the purge gas due to its high thermal conductivity. Hermetically sealed sample and reference aluminum pans, matched within 0.5 mg, were used to encapsulate the test samples with weights ranging between 10 and 25 mg. Pulse amplitudes between 1°C and 5°C, and durations between 1 and 10 min, were imposed on the system using the Jump and Equilibrate method segments. Enough time was allowed between consecutive pulses for the system to return to equilibrium at the initial temperature. Cooling was provided by the LNCA II liquid nitrogen cooling accessory.

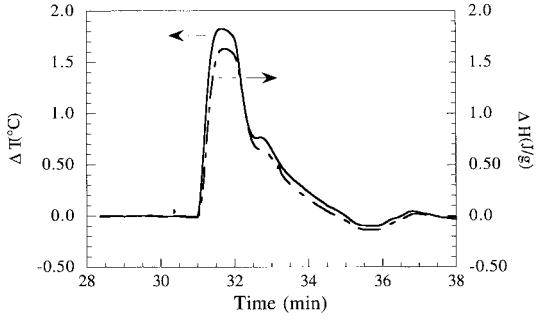

Fig. 1. A typical input temperature pulse and output enthalpy profile in a Pulse-DSC experiment.

Two sets of pulsed experiments were carried out on the pure hard and soft phases, and the blend with 50% hard phase. The first set involved introducing a set of different temperature pulses at a constant temperature (−50°C and 60°C, respectively) to measure the equilibrium specific heats in the glassy and rubbery states. A typical pulse in temperature and the resulting enthalpy is shown in Fig. 1.

In the second set, a single pulse was introduced at a series of temperatures as the sample was cooled through its glass transition. Enough time was allowed at each pre-determined temperature for equilibration. Fig. 2 shows a typical set of temperature pulses used to monitor the change of specific heat through the material's T_g. The pulsed data at each temperature was analyzed to yield the equilibrium specific heat.

3. Results and discussion

3.1. TGA of acrylic blends

Fig. 3 shows the loss in weight of pure hard and soft phases as well as the blend with 50% hard phase as a function of temperature. The onset of degradation, defined by the temperature of 10% weight loss, is

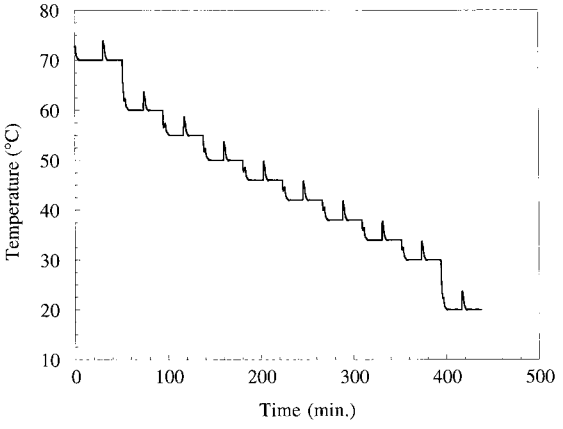

Fig. 2. Sequence of temperature pulses used during a cooling experiment to measure specific heat through T_g.

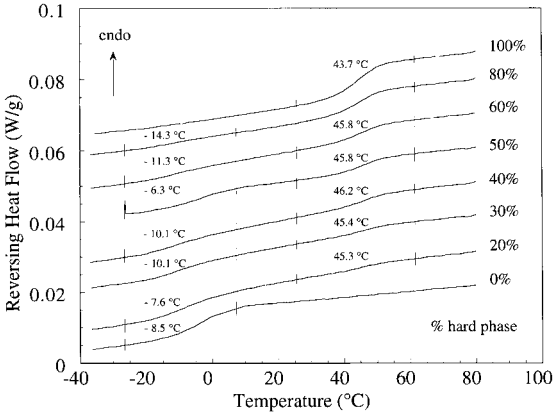

Fig. 4. Reversing heat flow vs. temperature for blend films. Curves have been shifted on *y*-axis by an arbitrary amount for clarity.

approximately 350–360°C. The degradation of these blends is quite rapid and involves nearly a 100% weight loss. This is as expected since the degradation of methylmethacrylate-based polymers approaches complete weight loss due to an unzipping reaction.

3.2. MDSC of acrylic blends

The profiles of reversing heat flow with temperature for blend compositions ranging from 0% hard to 100% hard phase are shown in Fig. 4. The curves have been shifted on the *y*-axis by an arbitrary amount to preserve clarity of presentation. Two distinct glass transitions corresponding to the pure hard and soft phases are seen throughout the entire range of blend compositions indicating phase separation of the two components. The size of the phase domains is much less than the range of wavelengths in visible light since the films are clear and transparent.

The glass transition temperatures, T_g, for the hard and soft phases in the blends were calculated by the mid-point method and are shown in Fig. 5. Also displayed are the peak temperatures in tan δ obtained from dynamic mechanical (DMTA) experiments. The

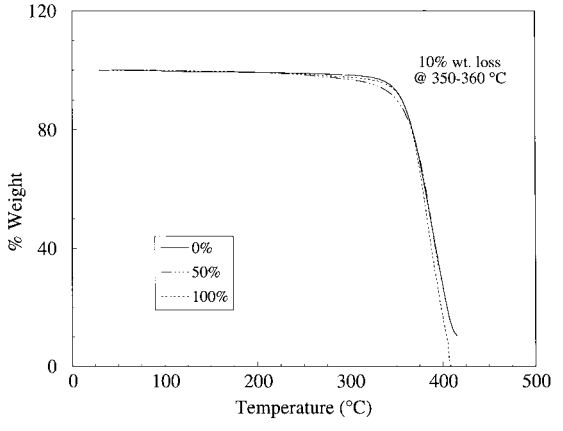

Fig. 3. TGA thermograms of pure hard and soft phases and the 50% hard blend at 10°C/min under nitrogen.

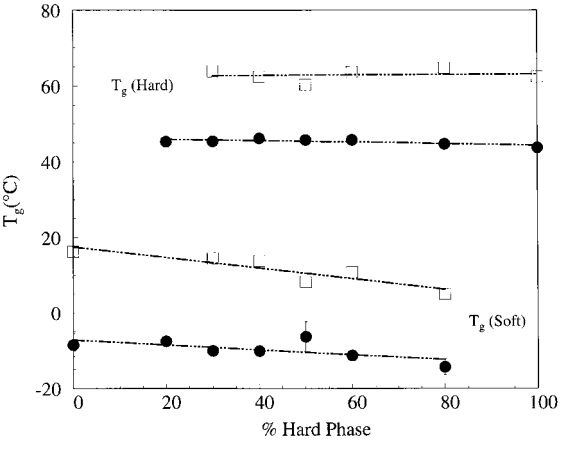

Fig. 5. Glass transition temperatures of the hard and soft phases for blends; circles show mid-point T_g from MDSC, squares show the peak tan δ values from DMTA.

T_g of the hard phase is not affected by the composition of the blend, whereas that of the soft phase shows a small depression upon increasing the concentration of the hard phase in the blend. A mismatch in thermal expansion coefficients between the hard and soft phases introduces an interfacial pressure as the blend is cooled from above the T_g. Using the pressure dependence of T_g for poly(methyl methacrylate) as a first approximation, Agarwal and Farris [6] estimated a depression of 3–10°C in the T_g of the soft phase. Similar results have been observed for blends of polystyrenes with rubber, such as ABS (acrylonitrile-butadiene-styrene), in which the T_g of the soft component (butadiene) is lowered by as much as 10°C due to the presence of the hard phase.

The height of the glass transition (change in specific heat, ΔC_p) is a characteristic parameter of any amorphous material. For blends, ΔC_p^{app} of each phase in the blended form relative to that in the pure component form, ΔC_p^0, is a measure of their miscibility. A non-dimensional ratio is defined as the relative heat capacity change for the blend

$$\Delta C_{p_{rel}} = \frac{w_1 \Delta C_{p_1}^{app} + w_2 \Delta C_{p_2}^{app}}{w_1 \Delta C_{p_1}^{0} + w_2 \Delta C_{p_2}^{0}}, \quad (9)$$

where w_1 and w_2 are the weight fractions of the blend constituents. A value of 1.0 for the above ratio indicates complete phase separation of the blend components. Fig. 6 shows the values of this ratio as a function of the blend composition. ΔC_p^{app} and ΔC_p^0 for each blend component were calculated from the difference of specific heat between the onset and end temperatures at its glass transition temperature in the blend and pure forms, respectively. The DSC2910 module software provided by TA instruments automatically calculates the onset and end points of a step transition by drawing tangents to the heat capacity curve in the rubbery and glassy region, and finding the intersection of a line drawn through the transition region with these tangents. Several start and end points were selected on the heat capacity curves to estimate the variability in the calculation of these onset and end points. A mean and a standard deviation in each of the ΔC_p^{app} and ΔC_p^0 values was calculated based on this variability, and applying the rules of propagation of errors for fractions, a net error for the $\Delta C_{p_{rel}}$ was estimated. The error bars in Fig. 6 show the net error calculated by this method.

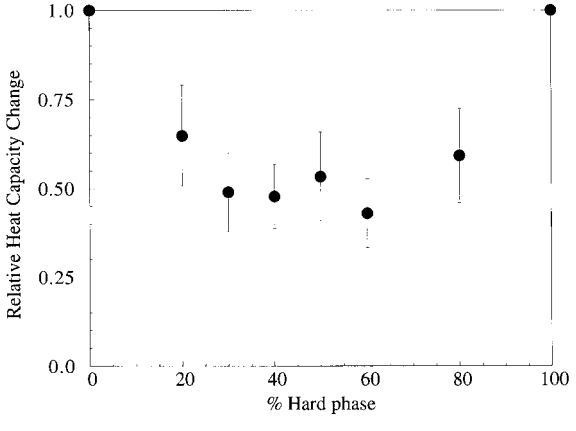

Fig. 6. Relative heat capacity change at T_g Eq. (9) for blends as a function of their composition.

There is increasing miscibility, indicated by values of relative heat capacity change of less than 1.0, upon increasing the hard phase. Initially, the matrix is a soft continuous phase with dispersions of the hard phase, and there is a considerable segmental inter-diffusion across the particle interface. As the concentration of the hard phase is increased, a percolation threshold is reached and the two phases exhibit a co-continuous morphology [6]. The value of the normalized specific heat is quite low (~0.5) at this point indicating substantial phase mixing. Upon further increase of the hard component, the matrix inverts to a continuous hard phase with dispersions of the soft phase. The profile of the normalized specific heat in Fig. 6 is symmetrical around 50% hard phase, indicating that the matrix inversion occurs around this composition.

A similar analysis has been applied by Fried [7] in his study on blends of poly(2,6-dimethyl-1,4-phenylene oxide) (PPO) and copolymers of styrene (S) and *p*-chlorostyrene (*p*ClS) which show a sharp transition from compatibility to incompatibility in a narrow range of copolymer compositions between 67.1 and 67.8 mol% *p*ClS. Blends of pure poly(*p*-chlorostyrene) (P*p*ClS) and PPO were totally incompatible and exhibited a value close to 1.0 for the normalized specific heat given by Eq. (9). The normalized specific heat values for blends of PPO with the copolymer containing 67.8 mol% *p*ClS were nearly 0.6 indicating considerable phase mixing in the interphase regions. Lower *p*ClS content in the copolymer resulted in

blends that were compatible, whereas higher *p*ClS content rendered the blends incompatible with normalized specific heats ranging from 0.7 to 1.0. A decrease in the specific heat change of the principal phases at the glass transition results in such blends, Fried argues, owing to the "depletion" of material in the interphase region, the weak contribution of which is not detectable in the DSC measurement. The degree to which the normalized specific heat is lower than 1.0 is a qualitative measure of partial blend miscibility.

The width of the glass transition, in a similar manner, is also a measure of relative blend miscibility. Widening of the glass transition temperature in a miscible blend has been understood to arise from the increasing microheterogeneity of the components [8–10] such that in the extreme case of incompatible blends, two separate transitions are seen. These suggestions are based on early work of Nielsen [11] on vinyl copolymers that showed a widening of logarithmic decrement in their mechanical spectra upon increasing heterogeneity between the components.

In case of compatible blends, Song et al. [10] have suggested a rule of mixtures type equation to explain the observed transition widths

$$\Delta T_{g,blend} = w_1 \Delta T_{g,1} + w_2 \Delta T_{g,2}, \tag{10}$$

where $\Delta T_{g,1}$ and $\Delta T_{g,2}$ are the widths of the glass transition temperatures of blend components in their pure form. However, for immiscible blend systems, an equation similar to Eq. (9) can be derived

$$\Delta T_{g_{rel}} = \frac{w_1 \Delta T_{g_1}^{app} + w_2 \Delta T_{g_2}^{app}}{w_1 \Delta T_{g_1}^{0} + w_2 \Delta T_{g_2}^{0}}, \tag{11}$$

where all the quantities have a corresponding description for the blend and the pure form.

Fig. 7 displays the absolute widths of glass transition temperatures of the soft and the hard phase in the blend as a function of blend composition in terms of the hard phase. These widths are estimated from the onset and end points, as in the case of specific heats described earlier, of the heat capacity curves. The error bars represent the uncertainty in the estimation of the onset and end points depending upon the choice of the pair of points selected for analysis of the transition. The width of each phase decreases as its concentration in the blend is decreased owing to its diminished presence as well as phase mixing in the interphase region. The normalized relative width at T_g, calculated by Eq. (11), and displayed in Fig. 8, shows a profile similar to that of the normalized specific heat of Fig. 6. Increased segmental inter-diffusion reduces the normalized relative width to values less than 1.0 and a minimum is seen around 40% consistent with the presence of a co-continuous phase morphology.

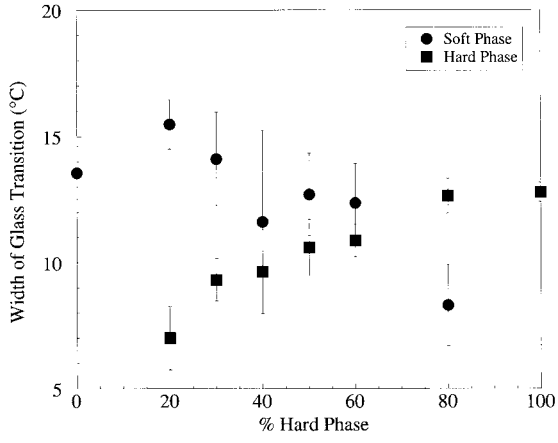

Fig. 7. Absolute values of the width of glass transition temperatures for the soft and the hard phases as a function of blend composition.

3.3. Pulsed-DSC on acrylic blends

3.3.1. Constant temperature experiments

In the first set of pulsed experiments on the pure hard and soft phases and the blend with 50% hard

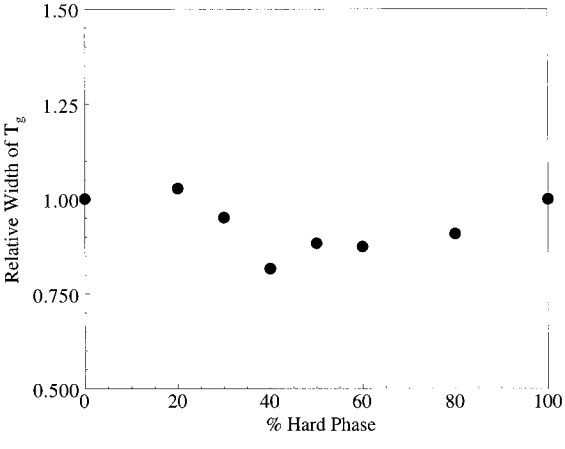

Fig. 8. Relative width of glass transition Eq. (11) for blends as a function of their composition.

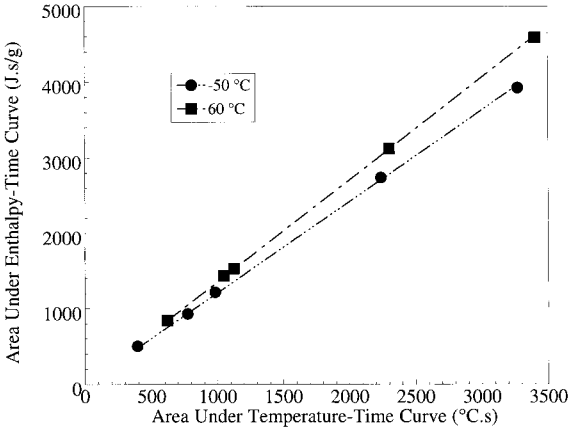

Fig. 9. Results of pulsed-DSC experiments on pure soft phase at −50°C and 60°C.

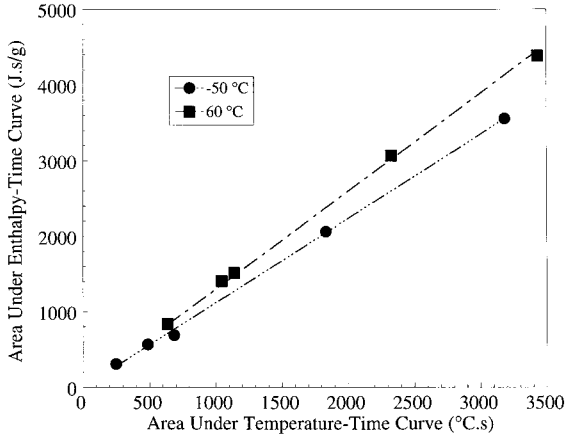

Fig. 11. Results of Pulsed-DSC experiments on pure hard phase at −50°C and 60°C.

phase, a series of temperature pulses of varying magnitudes and durations were introduced at a constant temperature. Figs. 9–11 show the results of these experiments at −50°C (glassy state) and 60°C (rubbery state). The linear dependence of the area under the enthalpy–time curve with that under the temperature–time curve is preserved over a large range of input pulse areas. The equilibrium specific heats in the glassy and rubbery states is calculated by the slope of a linear regression forced through the origin from this data. Table 1 summarizes the values of glassy and rubbery specific heats.

The change in specific heats through the glass transitions of the pure soft and hard phases are

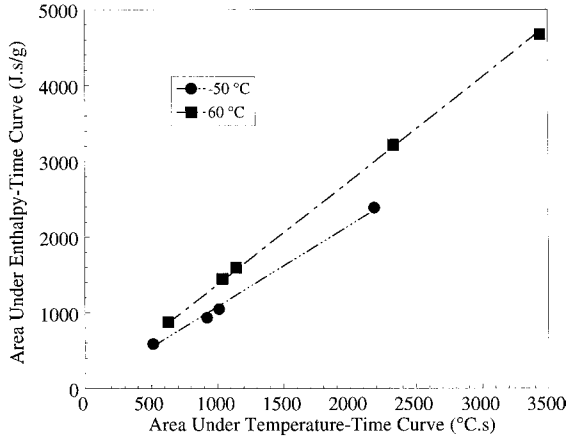

Fig. 10. Results of pulsed-DSC experiments on 50% hard phase blend at −50°C and 60°C.

0.1439 and 0.1801 J/g°C, respectively. It is interesting to note that the corresponding values obtained from MDSC experiments of Section 3.2 are higher at 0.1977 and 0.2664 J/g°C, respectively. The influence of the measurement frequency and cooling rate of the MDSC experiment on the values of specific heats is quite evident in these higher values.

3.3.2. *Experiments through T_g*

Figs. 12–14 show the variation of specific heat as a function of temperature as the sample is cooled from a rubbery state to the glassy state through its T_g. Each data point on the Pulsed-DSC profile is a result of a single pulse at that temperature. Also shown is the corresponding result from the MDSC experiments. A smooth curve through the pulsed-DSC data points in each case enables the estimation of a mid-point T_g by the half-width method.

These figures show that the change in specific heat through the glass transition is very accurately provided by the pulsed-DSC data. Further, both the mid-point T_g and the specific heat obtained from pulsed-DSC are

Table 1
Equilibrium specific heat, C_{eq}, calculated from the pulse experiments on acrylic blends

Material	Glassy C_{eq}	Rubbery C_{eq}
0% Hard	1.2097 ± 0.008	1.3536 ± 0.0039
50% Hard	1.0779 ± 0.019	1.3697 ± 0.008
100% Hard	1.1166 ± 0.012	1.2967 ± 0.012

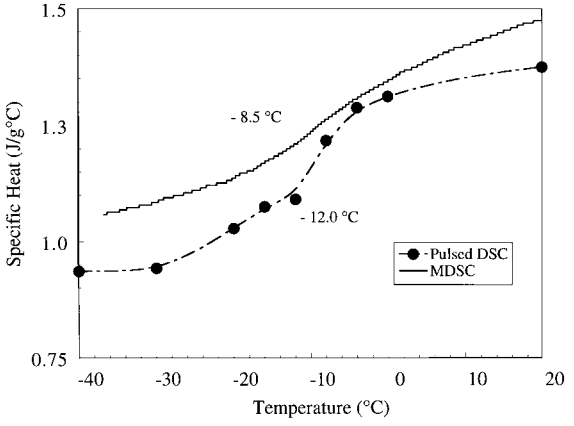

Fig. 12. Specific heat as a function of temperature for the pure soft phase measured by pulsed-DSC and MDSC.

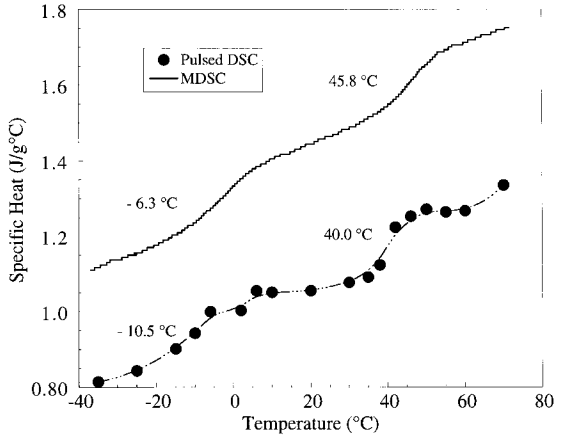

Fig. 14. Specific heat as a function of temperature for the 50% hard phase blend measured by pulsed-DSC and MDSC.

lower than the MDSC result. Once the change in input temperature and the output enthalpy has returned to the original unperturbed baseline value, analysis of the pulsed data using Eq. (8) yields a time-independent equilibrium specific heat. Pulsed-DSC, therefore, provides a rate-independent result which can be obtained from MDSC only in the limit of zero heating (or cooling) rate and zero frequency.

4. Conclusions

A detailed thermal characterization of the acrylic-based latex blend films has been carried out. These blends degrade rapidly at approximately 350°C. Reversing heat flow profiles from MDSC shows two distinct glass transition temperatures corresponding to each of the pure components indicating phase immiscibility. A normalized change in specific heat at T_g for each component in the blend with respect to that in the pure form, indicates partial miscibility arising from segmental inter-diffusion across the particle interface. A slight loss of this miscibility is seen at compositions approximately 50% hard phase, which corresponds to a matrix inversion from a soft to hard phase through a co-continuous phase morphology. The T_g of the hard phases is unaffected by the blend composition while that of the soft phase is depressed as the concentration of the hard phase increases.

Constant temperature pulsed-DSC experiments on the blends, as well as those through their T_g, show that the specific heats measured by MDSC are higher due to the influence of measurement frequency and the cooling rate. The variation of specific heat through T_g is very accurately measured by the pulsed-DSC method which also results in lower values for the glass transition temperatures. This technique, therefore, provides the rate-independent data which is not dependent on any kinetic factors.

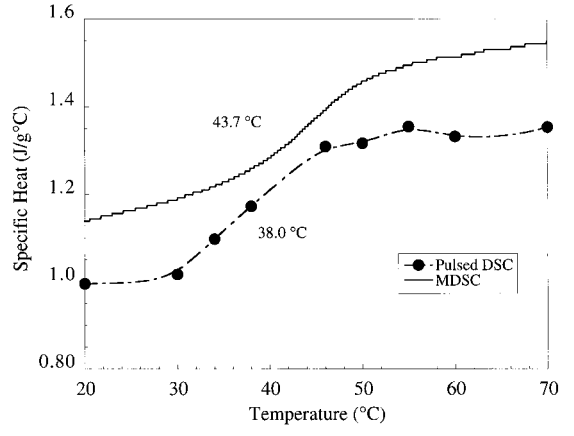

Fig. 13. Specific heat as a function of temperature for the pure hard phase measured by Pulsed-DSC and MDSC.

5. Nomenclature

$\Delta C_{p_{rel}}$ normalized specific heat change for incompatible blends (J/g°C)

ΔC_p^{app}	change in specific heat at the glass transition temperature in the blend (J/g°C)
ΔC_p^0	change in specific heat at the glass transition temperature in pure component form (J/g°C)
C_{eq}	equilibrium specific heat (J/g°C)
C'	in-phase component of complex specific heat
C'''	out-of-phase component of complex specific heat
$\|C\|$	modulus of the complex specific heat
H	enthalpy (J/g)
K_C	heat capacity constant obtained from sapphire calibrations in MDSC experiments
T	temperature (°C)
T_0	initial temperature in a MDSC experiment (°C)
T_a	amplitude of modulated temperature in MDSC T_g glass transition temperature (°C)
ΔT_g	width of glass transition temperature (°C)
$\Delta T_{g_{rel}}$	normalized width of the glass transition temperature for incompatible blend (°C)
$\Delta T_{g_i}^{app}$	width of glass transition for component i in the blend (°C)
$\Delta T_{g_i}^0$	width of glass transition for component i in pure form (°C)
t	time (s)
w_i	weight fraction of component i in the blend
β_0	heating rate in a DSC or MDSC experiment (°C/s)
ϕ	heat flux measured in a DSC or MDSC experiment (W/g)
ϕ_a	amplitude of oscillating heat flux measured in a MDSC experiment (W/g)
ϕ_{dc}	average heat flux in a MDSC experiment (W/g)
ϕ_{rev}	reversing heat flow in MDSC (W/g)
$\phi_{non\text{-}rev}$	non-reversing heat flow in MDSC (W/g)
φ	phase shift (rad)
ω_0	frequency of modulation in a MDSC experiment (rad/s)

Acknowledgements

The authors acknowledge the Materials Research Science and Engineering Center (MRSEC) at the University of Massachusetts, Amherst, for use of their research facilities. Financial support was provided by DuPont through the Center for University of Massachusetts Industry Research on Polymers (CUMIRP). We thank Dr. G.D. Andrews and Dr. S. Mazur of DuPont for synthesizing the latices and helpful discussions. This work forms a part of N. Agarwal's Ph.D. dissertation and he gratefully acknowledges the contribution of Dr. Mazur on his research committee.

References

[1] M. Reading, A. Luget, R. Wilson, Thermochim. Acta 238 (1994) 295–307.
[2] A. Boller, Y. Jin, B. Wunderlich, J. Thermal Anal. 42 (1994) 307–330.
[3] B. Wunderlich, J. Thermal Anal. 48 (1997) 207–224.
[4] J.E.K. Schawe, Thermochim. Acta 260 (1995) 1–16.
[5] N. Agarwal, R.J. Farris, J. Polym. Anal. Char. (1999), in press.
[6] N. Agarwal, R.J. Farris, Polym. Eng. Sci. (1998), in press.
[7] J.L. Fried, Ph.D. Thesis, University of Massachusetts Press, Amherst, MA, 1976.
[8] S.N. Cassu, M.I. Felisberti, Polymer 38(15) (1997) 3907.
[9] J.N. Clark, J.S. Higgins, C.K. Kim, D.R. Paul, Polymer 33(15) (1992) 3137.
[10] M. Song, A. Hammiche, H.M. Pollock, D.J. Hourston, M. Reading, Polymer 37(25) (1996) 5661.
[11] L.E. Nielsen, J. Amer. Chem. Soc. 75 (1953) 1435.